

COMPUTER SIMULATION OF A PARALLEL LINK MANIPULATOR

James D. Lee

James S. Albus

Nicholas G. Dagalakis

Tsungming Tsai

Robot Systems Division
National Bureau of Standards
Gaithersburg, MD 20899

ABSTRACT

A parallel link manipulator has been designed, which may be used as a robot wrist. The dynamic equations of the system have been formulated rigorously without assuming that the displacements and rotations are small. In computer simulation, it is shown that this manipulator can be used to perform tasks such as position control, path tracing, and force control. For each task, the control algorithm is formulated and tested.

INTRODUCTION

Most of today's industrial robots are built of successive links, usually hinged at rotary joints, which are actuated in a coordinated fashion to position the end-effector. In contrast to this configuration, the actuators/links assembled in the parallel link manipulator are not staged one atop the other and each link serves a role equal to its neighbors. Generally speaking, serial link manipulators have the advantage of access to large work spaces. On the other hand, parallel link manipulators are known for the simplicity of their mechanical design, and their high strength- and stiffness-to-weight ratios, because their actuators bear no moment loads but act in simple axial force. They are also known for their high force and moment capacity, since their actuators act all in parallel.

The parallel link manipulator is of interest in its own right, from the point of view of its design, kinematic analysis, dynamics, control, and performance. It can be used as a robot manipulator by itself and it can also be used as a robot wrist by attaching it to a robot arm. The idea of parallel link manipulator was first used for the design of flight simulators by Stewart [1]. With the increasing interest in robotic manipulators, studies have been conducted for its use as a mechanical wrist [2], a compliant device [3], a force/moment or position sensor [4], and a robot arm [5-11]. Recently, the Robot Systems Division at NBS has built, analyzed, and measured the stiffness of a six-cable robot crane suspension system [12-13]. Do and Yang have derived the dynamic equations and performed the inverse dynamic analysis and computer simulation of a Stewart platform [14].

In this paper a new design of parallel link manipulator is proposed. In this design, six identical pistons, each controlled independently by a hydraulic system, are used to connect two plates (platforms). The damping, as well as the compliance, of the system can be adjusted. The dynamic equations of the system are rigorously formulated without assuming that displacements and rotations involved are small. In this work, it is intended to demonstrate that this manipulator can be used for tasks such as position control, path tracing, and force control through computer simulation. For each task, the control algorithm is formulated and tested. For illustrative purpose, typical numerical results for each task are presented and discussed. In this work the manipulator is used as a stand alone device. For future research, it will be interesting to mount this parallel link manipulator as a wrist to a serial link robot arm and to study the involved issues of dynamics, control, and performance measures.

PROBLEM DESCRIPTION

The parallel link manipulator being considered in this work is shown in Fig. 1. The manipulator consists of (1) a lower plate which is fixed in space, (2) an upper plate which is movable with respect to the lower plate, and (3) six actuators which link the two plates together. In this work, the six actuators are considered to be six identical pistons, each can be controlled independently by a hydraulic system which will be described in a later section. Let the (x, y, z) coordinate system be fixed in space with the origin located at the center of the lower plate and the z -axis normal to the lower plate. Let the (α, β, γ) coordinate system be embedded in the upper plate. The γ -axis is normal to the upper plate and the origin of the (α, β, γ) coordinate system is located at the center of the upper plate. At reference state, the two plates are parallel, the orientation of the space axes coincides with that of the body axes, and the distance between the two plates is denoted by h .

The i -th piston ($i = 1, 2, 3, \dots, 6$) connects point a_i , on the lower plate, and point b_i , on the upper plate. The coordinates of a_i and b_i are

$$a_i: (x_i, y_i, z_i) = (r \cos \Gamma_i, r \sin \Gamma_i, 0), \quad (1)$$

$$b_i: (\alpha_i, \beta_i, \gamma_i) = (r \cos \Delta_i, r \sin \Delta_i, 0), \quad (2)$$

where

$$(\Gamma_1, \Gamma_2, \Gamma_3, \Gamma_4, \Gamma_5, \Gamma_6) = (10^\circ, 50^\circ, 130^\circ, 170^\circ, 250^\circ, 290^\circ), \quad (3)$$

$$(\Delta_1, \Delta_2, \Delta_3, \Delta_4, \Delta_5, \Delta_6) = (-10^\circ, 70^\circ, 110^\circ, 190^\circ, 230^\circ, 310^\circ). \quad (4)$$

TRANSFORMATION

The transformation from one cartesian coordinate system to another can be carried out by means of three translations and three successive rotations performed in a specific sequence. The Eulerian angles are then defined as the three successive angles of rotation. In this work, the sequence is started by rotating the upper plate by an angle ϕ about the γ -axis. Then the upper plate is rotated by an angle θ about the α -axis and, finally, by an angle ψ about the β -axis. Note that the first rotation and the second rotation are the same as those in Goldstein's treatment [15], however, the third rotation in Goldstein's treatment is a rotation of angle ψ

about the γ -axis. It can be shown that these two sets of Eulerian angles are equivalent in their capability to represent any specified rigid body rotation. Let u_x, u_y, u_z be the displacement components of the center of the upper plate. The space coordinates of a generic point on the upper plate, after it is rotated and displaced, may be obtained as

$$\begin{bmatrix} x \\ y \\ z \end{bmatrix} = \mathbf{P} \begin{bmatrix} \alpha \\ \beta \\ \gamma \end{bmatrix} + \begin{bmatrix} u_x \\ u_y \\ u_z + h \end{bmatrix}, \quad (5)$$

where $(\alpha, \beta, \gamma)^T$ is the body coordinates of that point and the transformation matrix, \mathbf{P} , can be expressed in terms of the three Eulerian angles as

$$\mathbf{P} = \begin{bmatrix} \cos\psi\cos\phi - \sin\psi\sin\theta\sin\phi & -\cos\theta\sin\phi & \sin\psi\cos\phi + \cos\psi\sin\theta\sin\phi \\ \cos\psi\sin\phi + \sin\psi\sin\theta\cos\phi & \cos\theta\cos\phi & \sin\psi\sin\phi - \cos\psi\sin\theta\cos\phi \\ -\sin\psi\cos\theta & \sin\theta & \cos\psi\cos\theta \end{bmatrix}. \quad (6)$$

LAGRANGE'S EQUATIONS

The components of the angular velocity, ω , along the body axes may be written as

$$\omega_\alpha = \dot{\theta}\cos\psi - \dot{\phi}\sin\theta\sin\psi, \quad (7)$$

$$\omega_\beta = \dot{\psi} + \dot{\phi}\sin\theta, \quad (8)$$

$$\omega_\gamma = \dot{\theta}\sin\psi + \dot{\phi}\cos\theta\cos\psi, \quad (9)$$

and the components of the linear velocity, v , along the space axes are simply

$$v_x = \dot{u}_x, \quad (10)$$

$$v_y = \dot{u}_y, \quad (11)$$

$$v_z = \dot{u}_z. \quad (12)$$

Let M and \mathbf{I} be the mass and the (mass) moment of inertia tensor of the upper plate, respectively, then the kinetic energy of the plate, T , is obtained as

$$T = \frac{1}{2} \{ M(v_x^2 + v_y^2 + v_z^2) + I_{\alpha\alpha}\omega_\alpha^2 + I_{\beta\beta}\omega_\beta^2 + I_{\gamma\gamma}\omega_\gamma^2 + 2I_{\alpha\beta}\omega_\alpha\omega_\beta + 2I_{\beta\gamma}\omega_\beta\omega_\gamma + 2I_{\gamma\alpha}\omega_\gamma\omega_\alpha \}. \quad (13)$$

Now consider the generalized coordinates, \mathbf{q} , and the generalized forces, \mathbf{Q} , to be, respectively,

$$\begin{aligned} \mathbf{q} &\equiv (q_1, q_2, q_3, q_4, q_5, q_6) \\ &= (u_x, u_y, u_z, \theta, \psi, \phi), \end{aligned} \quad (14)$$

$$\begin{aligned} \mathbf{Q} &\equiv (Q_1, Q_2, Q_3, Q_4, Q_5, Q_6) \\ &= (F_x, F_y, F_z, M_\theta, M_\psi, M_\phi). \end{aligned} \quad (15)$$

The generalized forces (forces and moments) may include the externally applied forces and moments and those due to the gravity and due to the forces exerted by the pistons. This

implicitly implies that the kinetic energy of the pistons has not been taken into account in this work.

The Lagrange's equations, which can be derived from either Hamilton's principle or D'Alembert's principle, can be written as [15]:

$$\frac{d}{dt} \left(\frac{\partial T}{\partial \dot{q}_i} \right) - \frac{\partial T}{\partial q_i} = Q_i, \quad i = 1, 2, \dots, 6. \quad (16)$$

Substituting eqn.(13) into eqn.(16), the following set of governing equations for the upper plate is obtained as

$$M\ddot{u}_x = F_x, \quad (17)$$

$$M\ddot{u}_y = F_y, \quad (18)$$

$$M\ddot{u}_z = F_z, \quad (19)$$

$$\begin{aligned} \dot{A}_\theta &- (I_{\alpha\alpha}\omega_\alpha + I_{\alpha\beta}\omega_\beta + I_{\alpha\gamma}\omega_\gamma) \dot{\phi} \sin\theta \sin\psi \\ &- (I_{\beta\alpha}\omega_\alpha + I_{\beta\beta}\omega_\beta + I_{\beta\gamma}\omega_\gamma) \dot{\phi} \cos\theta \\ &+ (I_{\alpha\gamma}\omega_\alpha + I_{\beta\gamma}\omega_\beta + I_{\gamma\gamma}\omega_\gamma) \dot{\phi} \sin\theta \cos\psi \\ &= M_\theta, \end{aligned} \quad (20)$$

$$\begin{aligned} \dot{A}_\psi &+ (I_{\alpha\alpha}\omega_\alpha + I_{\alpha\beta}\omega_\beta + I_{\alpha\gamma}\omega_\gamma) \omega_\gamma \\ &- (I_{\alpha\gamma}\omega_\alpha + I_{\beta\gamma}\omega_\beta + I_{\gamma\gamma}\omega_\gamma) \omega_\alpha \\ &= M_\psi, \end{aligned} \quad (21)$$

$$\dot{A}_\phi = M_\phi, \quad (22)$$

where

$$\begin{aligned} A_\theta &\equiv (I_{\alpha\alpha}\omega_\alpha + I_{\alpha\beta}\omega_\beta + I_{\alpha\gamma}\omega_\gamma) \cos\psi \\ &+ (I_{\alpha\gamma}\omega_\alpha + I_{\beta\gamma}\omega_\beta + I_{\gamma\gamma}\omega_\gamma) \sin\psi, \end{aligned} \quad (23)$$

$$A_\psi \equiv I_{\alpha\beta}\omega_\alpha + I_{\beta\beta}\omega_\beta + I_{\beta\gamma}\omega_\gamma, \quad (24)$$

$$\begin{aligned} A_\phi &\equiv - (I_{\alpha\alpha}\omega_\alpha + I_{\alpha\beta}\omega_\beta + I_{\alpha\gamma}\omega_\gamma) \cos\theta \sin\psi \\ &+ (I_{\alpha\beta}\omega_\alpha + I_{\beta\beta}\omega_\beta + I_{\beta\gamma}\omega_\gamma) \sin\theta \\ &+ (I_{\alpha\gamma}\omega_\alpha + I_{\beta\gamma}\omega_\beta + I_{\gamma\gamma}\omega_\gamma) \cos\theta \cos\psi. \end{aligned} \quad (25)$$

Note that M_θ , M_ψ , and M_ϕ are moments about the line of nodes, the body y -axis, and the space z -axis, respectively, while the line of nodes is defined to be the body x -axis before the rotation ψ takes place [15]. In terms of the moments about the space axes, M_θ , M_ψ , and M_ϕ can be expressed as

$$M_\theta = M_x \cos\phi + M_y \sin\phi, \quad (26)$$

$$M_\psi = -M_x \sin\phi \cos\theta + M_y \cos\phi \cos\theta + M_z \sin\theta, \quad (27)$$

$$M_{\phi} = M_z \quad (28)$$

Eqns.(26-28) can be rewritten as

$$M_x = M_{\theta} \cos\phi - M_{\psi} \sin\phi / \cos\theta + M_{\phi} \sin\phi \tan\theta \quad , \quad (26^*)$$

$$M_y = M_{\theta} \sin\phi + M_{\psi} \cos\phi / \cos\theta - M_{\phi} \cos\phi \tan\theta \quad , \quad (27^*)$$

$$M_z = M_{\phi} \quad . \quad (28^*)$$

If the principal axes of the upper plate coincide with the body axes, then all the off-diagonal terms in the inertia tensor (also named as products of inertia) vanish and the governing equations, eqns.(20-22), may be simplified significantly.

PISTON

The six pistons, which link the upper plate and the lower plate together, are identical. Each piston can be controlled independently. The piston and its hydraulic control system are schematically shown in Fig. 2. Consider that chambers 1,2,3 are filled with air and chambers 4,5 are filled with oil, which is assumed to be incompressible. The pressure in the i -th chamber is denoted by p_i ; f is named the piston force; A_i is the effective area of the cross section; V symbolically represents an orifice, which will provide damping to the system. It is assumed that the pressures, p_1 and p_4 , as well as the height of the second chamber, η , can be measured; and the height of the third chamber, δ , can be controlled. Obviously, the pressures in the second, the third, and the fifth chambers are related as

$$p_2 = p_3 \equiv p = p_5 A_5 / A_2 \quad , \quad (29)$$

and, by applying the ideal gas law, one obtains

$$p_1(L - \xi) = p_1^{\circ}(L - \xi^{\circ}) \quad , \quad (30)$$

$$p(A_2\eta + A_3\delta) = p^{\circ}(A_2\eta^{\circ} + A_3\delta^{\circ}) \quad , \quad (31)$$

where p° , p_1° , ξ° , η° , δ° stands for the value of p , p_1 , ξ , η , δ at the reference state, respectively. The governing equation for fluid flowing through the orifice can be expressed as [16]:

$$A_4 \dot{\xi} = A_5 \dot{\eta} = \text{sign}(p_5 - p_4) \sqrt{|p_5 - p_4|} / \beta_1 \quad (32a)$$

for turbulent flow, and

$$A_4 \dot{\xi} = A_5 \dot{\eta} = (p_5 - p_4) / \beta_2 \quad (32b)$$

for laminar flow, where β_1 and β_2 are constants to be determined experimentally. The piston force is balanced by the difference between pressure induced forces in the first chamber and the fourth chamber, i.e.,

$$f + p_1 A_1 = p_4 A_4 \quad . \quad (33)$$

Note that, in the reference state,

$$p_1^{\circ} A_1 = p_4^{\circ} A_4 = p_5^{\circ} A_4 = p^{\circ} \frac{A_2}{A_5} A_4 \quad .$$

Combining eqns.(29-33), one may obtain the governing equation for the piston as

$$f = A_4 \left\{ -D[\dot{\xi}] + \frac{A_2}{A_5} p^o K[\xi, \delta] \right\} , \quad (34)$$

where

$$D[\dot{\xi}] \equiv \begin{cases} (A_4 \dot{\xi} \beta_1)^2 \text{sign}(\dot{\xi}) & , \quad (\text{turbulent flow}) \\ A_4 \dot{\xi} \beta_2 & , \quad (\text{laminar flow}) \end{cases} \quad (35a)$$

$$K[\xi, \delta] \equiv \frac{A_2 \eta^o + A_3 \delta^o}{A_2 \eta^o + A_3 \delta + A_2 A_4 (\xi - \xi^o) / A_5} - \frac{L - \xi^o}{L - \xi} . \quad (36)$$

The total length of the piston, l , is equal to the height of the fourth chamber, ξ , plus a constant, i.e.,

$$l = \xi + C . \quad (37)$$

However, ξ is related to η as

$$\xi = \frac{A_5}{A_4} (\eta - \eta^o) + \xi^o . \quad (38)$$

Eqns.(37,38) imply that the total length of the piston can be measured since η is measurable. Eqn.(33) implies that the piston force can be measured since p_1 and p_4 are measurable. Then the governing equation of the piston can be symbolically written as

$$f = f(l, \dot{l}, \delta) . \quad (39)$$

For illustrative purpose, the numerical values of all the relevant parameters used in this work are listed as follows:

$r = 2 \text{ in.}$	$h = 3 \text{ in.}$
$A_1 = 0.3518 \text{ in.}^2$	$A_2 = 1.6085 \text{ in.}^2$
$A_3 = 2.0106 \text{ in.}^2$	$A_4 = 0.5026 \text{ in.}^2$
$A_5 = 2.0106 \text{ in.}^2$	$L = 4 \text{ in.}$
$\xi^o = 2 \text{ in.}$	$\eta^o = 2 \text{ in.}$
$\delta^o = 4 \text{ in.}$	$C = 1.0794 \text{ in.}$
$p^o = 100 \text{ psi}$	$M = 2 \text{ lb}$

and the nonvanishing components of the (mass) moment of inertia tensor are

$$I_{\alpha\alpha} = I_{\beta\beta} = 2 \text{ lb-in.}^2$$

$$I_{\gamma\gamma} = 4 \text{ lb-in.}^2$$

The compliance of the piston may be demonstrated by a plot of $-f$ vs $\Delta\xi \equiv \xi - \xi^o$ (a force-displacement curve) with $\Delta\delta \equiv \delta^o - \delta$ being the parameter in Fig.3. It is seen that $-f$

approaches infinity as $\Delta\xi$ approaches 2 inches (equivalent to $\xi \rightarrow L$) because the air in the first chamber is assumed to follow the ideal gas law. There is a lower limit for $\Delta\xi$ at -2 inches (equivalent to $\xi = 0$) where the piston force is indeterminate -- at that limiting value, the piston becomes infinite rigid. The damping of the piston may be demonstrated by a plot of $\Delta\xi$ vs. time, i.e., solve eqn.(34) with $f = 0$, $\delta = \delta^0$, and the initial condition $\Delta\xi = 1$ in. at $t = 0$. The solutions of eqn.(34) are plotted in Fig.4 for different values of β_2 . The larger the value is for β_2 the longer it takes for $\Delta\xi$ to be reduced to zero. The unit for β_2 is *psi -sec. / in.³*.

GENERALIZED FORCES

The i -th piston connects point $a_i(x_i, y_i, z_i)$, on the lower plate, and point b_i on the upper plate. When the upper plate assumes the generalized coordinates $q = (u_x, u_y, u_z, \theta, \psi, \phi)$, the space coordinates of the point b_i become x_i^* where

$$x_i^* = \begin{bmatrix} x_i^* \\ y_i^* \\ z_i^* \end{bmatrix} = P \begin{bmatrix} r \cos \Delta_i \\ r \sin \Delta_i \\ 0 \end{bmatrix} + \begin{bmatrix} u_x \\ u_y \\ u_z + h \end{bmatrix}. \quad (40)$$

The unit vector from point a_i to point b_i is

$$e_i = \left(\frac{x_i^* - x_i}{l_i}, \frac{y_i^* - y_i}{l_i}, \frac{z_i^* - z_i}{l_i} \right), \quad (41)$$

where l_i is the length of i -th piston, i.e.,

$$l_i = \sqrt{(x_i^* - x_i)^2 + (y_i^* - y_i)^2 + (z_i^* - z_i)^2}. \quad (42)$$

The i -th piston force acting on the upper plate is

$$f_i = f_i e_i$$

where f_i , according to eqn.(39), is a function of the length, l_i , the time derivative of the length, \dot{l}_i , and the control variable, δ_i . From eqn.(42), the time derivative of the length can be derived as

$$\dot{l}_i = [(x_i^* - x_i)\dot{x}_i^* + (y_i^* - y_i)\dot{y}_i^* + (z_i^* - z_i)\dot{z}_i^*] / l_i, \quad (43)$$

and, from eqn.(40), $(\dot{x}_i^*, \dot{y}_i^*, \dot{z}_i^*)$ can be obtained as

$$\begin{bmatrix} \dot{x}_i^* \\ \dot{y}_i^* \\ \dot{z}_i^* \end{bmatrix} = \dot{P} \begin{bmatrix} r \cos \Delta_i \\ r \sin \Delta_i \\ 0 \end{bmatrix} + \begin{bmatrix} \dot{u}_x \\ \dot{u}_y \\ \dot{u}_z \end{bmatrix}. \quad (44)$$

The forces acting on the upper plate by the six pistons can be expressed as

$$f = \sum_{i=1}^6 f_i e_i. \quad (45)$$

The moments acting on the upper plate due to the six piston-forces are obtained as

$$\mathbf{m} = \sum_{i=1}^6 \mathbf{r}_i \times f_i \mathbf{e}_i , \quad (46)$$

where \mathbf{r}_i is the i -th moment arm (a vector from the center of the upper plate to point b_i) which can be calculated as

$$\mathbf{r}_i = Pr \begin{bmatrix} \cos\Delta_i \\ \sin\Delta_i \\ 0 \end{bmatrix} . \quad (47)$$

POSITION CONTROL

One of the basic tasks for a robot to perform is to place its end-effector at a desired location and orientation, which may be called the target position. For a given target position, it is straightforward to figure out the final generalized coordinates of the upper plate, $\hat{\mathbf{q}} \equiv \{ \hat{u}_x, \hat{u}_y, \hat{u}_z, \hat{\theta}, \hat{\psi}, \hat{\phi} \}$. In other words, if

$$\lim_{t \rightarrow \infty} \mathbf{q}(t) = \hat{\mathbf{q}} , \quad (48)$$

then the end-effector will reach the target position and stay there. Using eqns.(40,42) with the substituting of $\mathbf{q} = \hat{\mathbf{q}}$, one may find the desired length of the pistons, $\hat{l}_i (i=1,2,3,\dots,6)$, and $\hat{\xi}_i (i=1,2,3,\dots,6)$, which is equal to $\hat{l}_i - C$ (eqn.(37)). The mapping from the generalized coordinates to the piston lengths is named inverse kinematics. Hence, the mapping from the piston lengths to the generalized coordinates is named forward kinematics. For parallel link manipulator, it is straightforward to perform the inverse kinematics but it takes an iterative numerical procedure to perform the forward kinematics. Let the inverse kinematics and the forward kinematics be represented, respectively, as

$$\mathbf{L} = \mathbf{G}^{-1}(\mathbf{q}) , \quad (49)$$

$$\mathbf{q} = \mathbf{G}(\mathbf{L}) , \quad (50)$$

where

$$\mathbf{L} \equiv (l_1, l_2, l_3, l_4, l_5, l_6) . \quad (51)$$

Similarly, let the mapping from the piston forces, $\mathbf{f} \equiv (f_1, f_2, f_3, f_4, f_5, f_6)$ to its resultant forces and moments, $\mathbf{F} \equiv (F_x, F_y, F_z, M_x, M_y, M_z)$ at a specific generalized coordinates, be represented as

$$\mathbf{F} = \mathbf{H}(\mathbf{f}, \mathbf{q}) . \quad (52)$$

This mapping may be named as forward-force-kinematics. Therefore the inverse-force-kinematics may be represented as

$$\mathbf{f} = \mathbf{H}^{-1}(\mathbf{F}, \mathbf{q}) . \quad (53)$$

It is straightforward to perform the forward-force- kinematics but it takes an iterative numerical procedure to perform the inverse-force-kinematics.

If the task is for the end-effector to reach a desired position and orientation characterized by $\hat{\mathbf{q}}$ with *a priori* knowledge of the externally applied forces and moments, including those

due to gravity, $F^a \equiv (F_x^a, F_y^a, F_z^a, M_x^a, M_y^a, M_z^a)$, then the control algorithm may be simply represented by the following procedures:

(1) Calculate the desired piston lengths by performing the following inverse kinematics

$$\hat{L} = G^{-1}(\hat{q}) . \quad (54)$$

(2) As the generalized coordinates of the manipulator approach \hat{q}^0 asymptotically, the time derivatives of all the variables approach zero. In other words, the total generalized forces, Q , approach zero and therefore

$$\lim_{t \rightarrow \infty} F = -F^a . \quad (55)$$

Then the desired piston forces may be calculated as

$$\hat{f} = H^{-1}(-F^a, \hat{q}) . \quad (56)$$

(3) The control law may be written as

$$K[\xi_i, \delta_i] = \hat{f}_i A_5 / A_2 A_4 p^0 , \quad (57)$$

which implies that the control variable $\delta_i (i=1,2,\dots,6)$ can be calculated as

$$\delta_i = \frac{R \eta^0 + \delta^0}{\hat{f}_i / f^0 + [(L - \xi^0) / (L - \xi_i)]} - R \eta^0 - f^0 (\xi_i - \xi^0) / A_3 p^0 , \quad (58)$$

where

$$R \equiv A_2 / A_3 , \quad f^0 \equiv p^0 A_2 A_4 / A_5 .$$

Because the control device of the manipulator involves the fluid flowing through the orifice, which is governed by eqn.(32a) or eqn.(32b), this system has an energy dissipation mechanism -- in fact β_1 or β_2 may be called the damping coefficient. Therefore, one can prove theoretically or numerically that, by setting the control variable δ_i to the value $\hat{\delta}_i$, the end-effector will reach the specified target and the settling time is inversely proportional to the magnitude of the damping coefficient.

However, it is more desirable to formulate the control algorithm for position control without *a priori* knowledge of the externally applied forces and moments because then the range of application is broader. For example, if the manipulator is commanded to pick up some objects and distribute them to several specified places, one does not have detailed information about the weights of those objects. For these applications, it is proposed to achieve position control through the following procedures:

(1) Calculate the desired piston lengths from eqn.(54).

(2) Set the control variable $\delta_i (i=1,2,\dots,6)$ to be δ^0 and activate the manipulator including the measurements of the piston lengths and forces. The settling time, t^* , is define to be the time beyond which all the variables, especially the piston lengths, reach their steady state values, i.e.,

$$|l_i^* - l_i(t)| < \epsilon \quad \text{for } t > t^* , \quad (59)$$

where $l_i^* (i=1,2,3,\dots,6)$ is the length of the i -th piston at $t=t^*$, and ϵ is the specified allowable

error.

(3) Calculate the following quantities in order

$$\begin{aligned} \mathbf{q}^* &= \mathbf{G}(\mathbf{L}^*) , \\ \mathbf{F} &= \mathbf{H}(\mathbf{f}^*, \mathbf{q}^*) , \\ \hat{\mathbf{f}} &= \mathbf{H}^{-1}(\mathbf{F}, \mathbf{q}) , \end{aligned} \quad (60)$$

where \mathbf{f}^* is the measured piston force at $t=t^*$, and \mathbf{F} is the calculated force and moment due to the measured piston forces.

(4) The control variable δ_i can now be calculated using eqn.(58).

The simulated computer results are shown in Fig.5 and Fig.6, in which the generalized coordinates, \mathbf{q} , are plotted as functions of time.

PATH TRACING

In this section, consider the end-effector a pin of length L_p , i.e., the position of the tip of the pin is $(0,0,L_p)$ in the (α,β,γ) coordinate system. The task is for the pin to trace a specified curve in space within a given duration. In other words, the tip of the pin has to reach (x_i, y_i, z_i) at $t=t_i$ ($i=1,2,3, \dots, n$).

For illustrative purpose, consider that the curve to be traced in space is a circle which can be expressed as :

$$\begin{aligned} x &= R_p \cos(2\pi t/T) , \\ y &= R_p \sin(2\pi t/T) , \\ z &= h + H , \end{aligned} \quad (61)$$

where the radius, R_p ; the height, H ; and the period, T ; are specified. There is redundancy involved in the task of path tracing because the manipulator has six degrees of freedom and a curve in space is only three dimensional. Besides, rotation about the axis of the pin does not affect the path traced by the pin.

In order to eliminate the redundancy, first let the center of the upper plate, $(\alpha=0,\beta=0,\gamma=0)$, trace a circle specified as follows :

$$\begin{aligned} x_c &= R_c \cos(2\pi t/T) , \\ y_c &= R_c \sin(2\pi t/T) , \\ z_c &= H + h - \sqrt{L_p^2 - (R_p - R_c)^2} . \end{aligned} \quad (62)$$

One may easily verify that the distance between (x, y, z) , from eqn.(61), and (x_c, y_c, z_c) is equal to the length of the pin, L_p . One way to eliminate the redundancy associated with the rotation about the axis of the pin is to set one of the three Eulerian angles to be zero. In this work, let $\phi = 0$, and then the other Eulerian angles are calculated to be

$$\bar{\psi} = \sin^{-1} \left[\frac{R_p - R_c}{L_p} \cos(2\pi t/T) \right] , \quad (63)$$

$$\bar{\theta} = -\sin^{-1} \left[\frac{R_p - R_c}{L_p} \sin(2\pi t/T) / \cos\psi \right] . \quad (64)$$

The desired generalized coordinates of the upper plate of the manipulator at time t can be written as

$$\bar{q}(t) = \{ x_c, y_c, H - \sqrt{L_p^2 - (R_p - R_c)^2}, \bar{\theta}, \bar{\psi}, 0 \} . \quad (65)$$

Then the desired piston lengths at time t can be calculated by performing the following inverse kinematics

$$\bar{L}(t) = G^{-1}(\bar{q}(t)) . \quad (66)$$

With the assumption that there is no externally applied loading, the control variable of the i -th piston at time t may be obtained as (cf. eqn.(58)):

$$\bar{\delta}_i(t) = \frac{(R\eta^0 + \delta^0)(L - \bar{\xi}_i)}{L - \xi^0} - R\eta^0 - f^0(\bar{\xi}_i - \xi^0) / A_3 p^0 , \quad (67)$$

where $\bar{\xi}_i = \bar{L}_i(t) - C$.

It is proposed to achieve path tracing through the following procedures :

- (1) Select a time interval, Δt , which may be named as the cycle time.
- (2) Between time $t_1 = t' - \Delta t$ and time $t_2 = t'$, calculate $\bar{q}(t_2)$, $\bar{L}(t_2)$, and $\bar{\delta}_i(t_2)$ ($i=1,2, \dots, 6$) using eqns.(65-67) and set the control variables to be $\bar{\delta}_i(t_2)$ for $t \in [t_1, t_2]$.

The performance of the manipulator to trace a path can be measured as follows: First, the difference between the desired position, (x, y, z) from eqn.(61), and the actual (simulated) position, (x', y', z') , at time t can be calculated as

$$e(t) = \{ [x(t) - x']^2 + [y(t) - y']^2 + [z(t) - z']^2 \}^{1/2} . \quad (68)$$

For the time period $[t_i, t_f]$, the index of performance measure, I , is defined as

$$I \equiv \frac{1}{(t_f - t_i) R_p} \int_{t_i}^{t_f} e(t) dt . \quad (69)$$

The simulated computer results are plotted in Fig.7 and Fig.8. In Fig.7, it is not surprising to find that the manipulator performs better (the index of performance measure is smaller) for larger period (the angular velocity to trace the circle is smaller). In Fig.8, the performance of the manipulator is seen as a function of the damping coefficient, β_2 . This function has an optimum when the damping coefficient is at certain value.

FORCE CONTROL

In this case let the end-effector of the manipulator be a pin of length L_p , as described in the previous case. The task is for the end-effector to touch a surface (in this work it is simplified to be a plane) and exert a force of specified amount normal to that surface. Assume that the robotic manipulator has no *a priori* knowledge of the position and orientation of the plane. The plane is characterized by

$$a_x x + a_y y + a_z z + d = 0 \quad , \quad (70)$$

where (a_x, a_y, a_z) is the unit normal of the plane, and d is the distance between the origin and the plane. If (x_p, y_p, z_p) is the coordinate of the tip of the pin, then the distance between (x_p, y_p, z_p) and the plane is

$$D = a_x x_p + a_y y_p + a_z z_p + d \quad . \quad (71)$$

Further assume that the plane is smooth so that the contact force, F , is always normal to the plane, i.e., friction is neglected in this study. If the plane is an ideally rigid plane, then the distance, D , must always be greater than or equal to zero and

$$F = 0 \quad \text{if } D > 0 \quad , \quad (72)$$

$$F = \text{unknown} \quad \text{if } D = 0 \quad , \quad (73)$$

where $F = \text{unknown}$ means that the contact force has to be determined by the state of the manipulator, not by the geometric relation between the pin and the plane. However, the contact problem represented by eqns.(72,73) is difficult to model, to say the least. In this work, instead, an elastic plane is modeled as follows:

$$F = 0 \quad \text{if } D \geq D_0 \quad , \quad (74)$$

$$F = -kD + F_0 \quad \text{if } D < D_0 \quad , \quad (75)$$

where k is the spring constant (usually set to be a very large value) of the elastic plane, F_0 is the desired force to be exerted on the plane, and $D_0 = F_0 / k$. In this work, k is set at 1000 lbf/inch. Now the force acting on the tip of the pin, in the vector form, can be expressed as

$$\mathbf{F} = (F a_x, F a_y, F a_z) \quad . \quad (76)$$

To achieve force control:

(1) Set the control variables at certain properly chosen values so that the end-effector will approach the plane slowly (by adjusting the damping coefficient to a relative large value). This step is equivalent to a position control without external forces and moments acting on it (however, one may include those due to gravity on the manipulator).

(2) when the end-effector encounters the plane, chattering phenomenon may be observed. After the chattering becomes less pronounced, at time $t=t_1$, calculate the following quantities in order:

$$\mathbf{q}(t_1) = \mathbf{q}_1 = \mathbf{G}(\mathbf{L}(t_1)) \quad , \quad (77)$$

$$\mathbf{F}(t_1) = \mathbf{F}_1 = \mathbf{H}(\mathbf{f}(t_1), \mathbf{q}(t_1)) \quad , \quad (78)$$

where \mathbf{F}_1 is the force and moment due to the measured piston forces at $t=t_1$. From \mathbf{F}_1 one can readily calculate the contact force, F_1 , at $t=t_1$. Then calculate the desired piston forces, \mathbf{f}_2 , as follows :

$$\mathbf{f}_2 = \mathbf{f}(t_1) F_0 / F_1 \quad . \quad (79)$$

Based on $l(t_1)$ and f_2 , one may calculate the desired control variables δ_2 by using eqn.(58).

(3) The control variables $\delta(t)$ at any time $t \in [t_1, t_f]$ are set to be

$$\delta(t) = \frac{\delta_1(t_f - t) + \delta_2(t - t_1)}{t_f - t_1}, \quad (80)$$

where t_f is the selected time when the contact force is supposed to reach F_0 . However, it is better to repeat Step 2 and Step 3 several times as long as $t_1 < t_f$.

(4) To make sure that the contact force is stabilized at F_0 after $t > t_f$, let the controller go through the calculation in Step 2 and Step 3 except that t_f should now be replaced by $t_1 + T$, where T is a properly selected time value.

From the computer simulated results, the distance D and the contact force F as functions of time are shown in Fig. 9 and Fig. 10. The damping coefficient is set at 20 psi-sec/in.^3 (5 psi-sec/in.^3) for the case shown in Fig. 9 (Fig. 10). Notice that the chattering phenomenon is reflected in Fig. 10.

DISCUSSION

The general form of dynamic equations for a parallel link manipulator has been obtained as eqns.(17 - 28). The actuators designed in this work are six identical pistons controlled by a hydraulic system. For a specific control variable, the piston acts like a one-dimensional, non-linear viscoelastic rod whose stiffness and damping can be adjusted. By changing the control variable, within a reasonable range, any specified piston force and piston length can be achieved. With properly chosen control algorithms, this parallel link manipulator can be used to perform tasks such as position control, path tracing, and force control. In position control, the end-effector can reach and stabilize at a target position with specified generalized coordinates even without *a priori* knowledge of the externally applied forces and moments -- a much needed capability in robotic assembly tasks. In path tracing, the manipulator performs better if the specified traveling speed of the end-effector is smaller and, by properly choosing the damping coefficient, we can make the manipulator achieve its optimum performance.

It is very common to observe chattering phenomena when a machine tool is brought into contact with a workpiece or a solid surface. However, it has been shown that the chattering phenomena may be eliminated when the damping coefficient becomes larger -- this can be achieved by adjusting the orifice area in the hydraulic control system [16]. Position control and force control can be combined and, by setting the contact force F_0 at a small value, one may use the manipulator in an uncertain environment and avoid damage done by and to the manipulator.

REFERENCES

- [1] Stewart, D., "A Platform with Six Degrees of Freedom", Proc. of the Inst. of Mech. Eng., Vol. 180, Part I, No. 15 pp.371-386, 1965-1966.

- [2] Bennett, W. M., "Mechanical Wrist for a Robot Arm", Mech. Eng. Dept., Mass. Inst. of Tech., B.S. Thesis, 1968.
- [3] McCallion, H., Johnson, G. R., Pham, D. T., "A Compliant Device for Inserting a Peg in a Hole", *The Industrial Robot*, pp.81-87, June 1979.
- [4] Koliskor, A. S., "Development and Investigation of Industrial Robots Based on Specification by 1-coordinates", *Soviet Engineering Research*, Vol.2, No.12, pp.75-78, 1982.
- [5] Fichter, E. F., McDowell, E. D., "A Novel Design for a Robot Arm", *Proc. Int. Computer Tech. Conf.*, pp. 250-256, Aug. 1980, San Francisco, California.
- [6] Fichter, E. F., "Kinematics of a Parallel Connection Manipulator", ASME Paper 84-DET-45 delivered at the Design Eng. Tech. Conf., Oct. 1984, Cambridge, Massachusetts.
- [7] Fichter, E. F., "A Stewart Platform Based Manipulator: General Theory and Practical Construction", *The Kinematics of Robot Manipulators*, MIT Press, pp.165-190, 1987.
- [8] Powell, I. L., "The Kinematic Analysis and Simulation of the Parallel Topology Manipulator", *The Marconi Review*, Vol.XLV, No.226, pp.121-138, 3rd quarter 1982.
- [9] Landsberger, S. E., Sheridan, T. B., "A New Design for Parallel Link Manipulators", *Proc. Systems Man and Cybernetics Conf.*, pp.812-814, Nov.1985, Tuscon, Arizona.
- [10] Sheridan, T. B., "Human Supervisory Control of Robot Systems", *Proc. Int. Conf. on Robotics and Automation*, pp.808-812, Apr. 1986, San Francisco, California.
- [11] Konstantinov, M. S., Sotirov, Z. M., Zamanov, V. B., Nenchev, D. N., "Force Feedback Control of Parallel Topology Manipulating Systems", *Proc. 15th Int. Symp. on Industrial Robots*, pp.181-188, Sep.1985, Tokyo, Japan.
- [12] Dagalakis, N. G., Albus, J. S., Wang, B. L., Unger, J., Lee, J. D., "Stiffness Study of a Parallel Link Robot Crane for Shipbuilding Applications", *Proc. of the 7th Int. Conf. on Offshore Mechanics and Arctic Engineering*, pp.29-37, February, 1988, Houston, Texas.
- [13] Albus, J. S., Dagalakis, N. G., Wang, B. L., Unger, J., Lee, J. D., Yancey, C. W., "Available Robotics Technology for Applications in Heavy industry", *Iron and Steel Engineer Magazine* (in press).
- [14] Do, W. Q. D., Yang, D. C. H., "Inverse Dynamic Analysis and Simulation of a Platform Type of Robot", *J. of Robotic Systems*, Vol.5, No.3, pp.209-227, 1988.
- [15] Goldstein, H., *Classical Mechanics*, Addison-Wesley Publishing Company, Reading, Massachusetts, 1950.
- [16] Ogata, K., *System Dynamics*, Prentice-Hall, Inc., Englewood Cliffs, New Jersey, 1978.

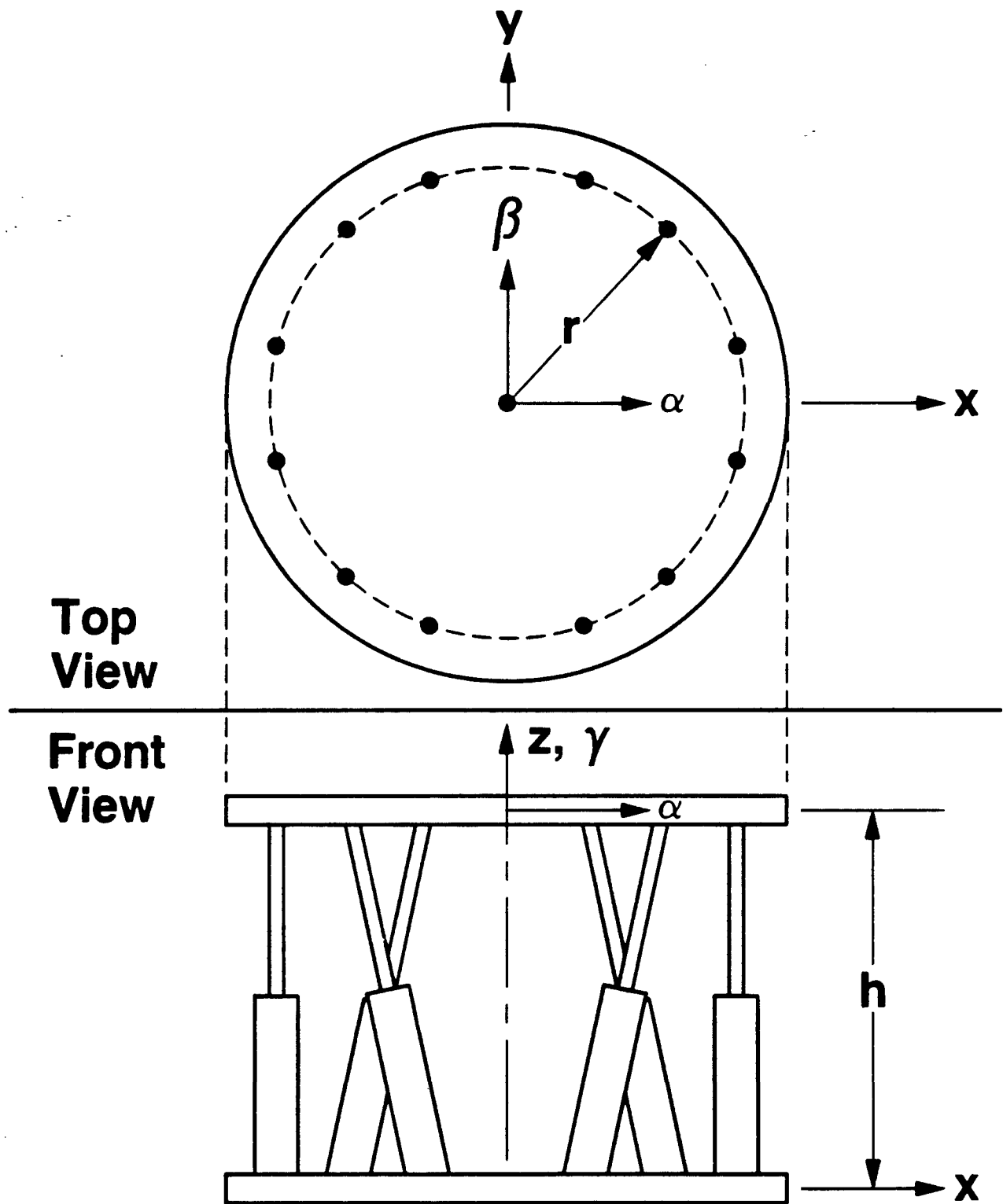


Figure 1. The Parallel Link Manipulator, in its Reference State, and The Coordinate Systems

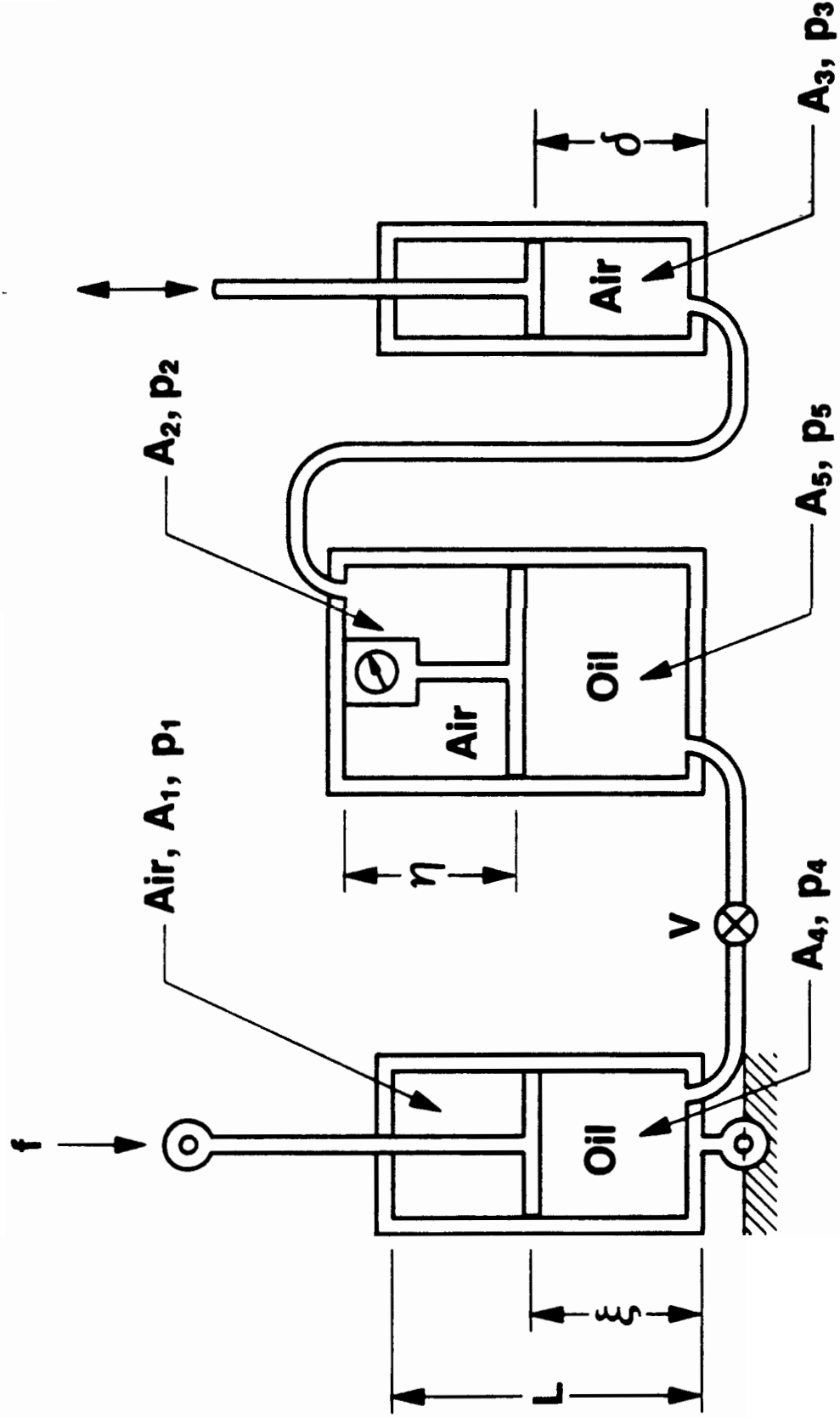


Figure 2. The Schematic Diagram of the Hydraulic Control System of the Piston

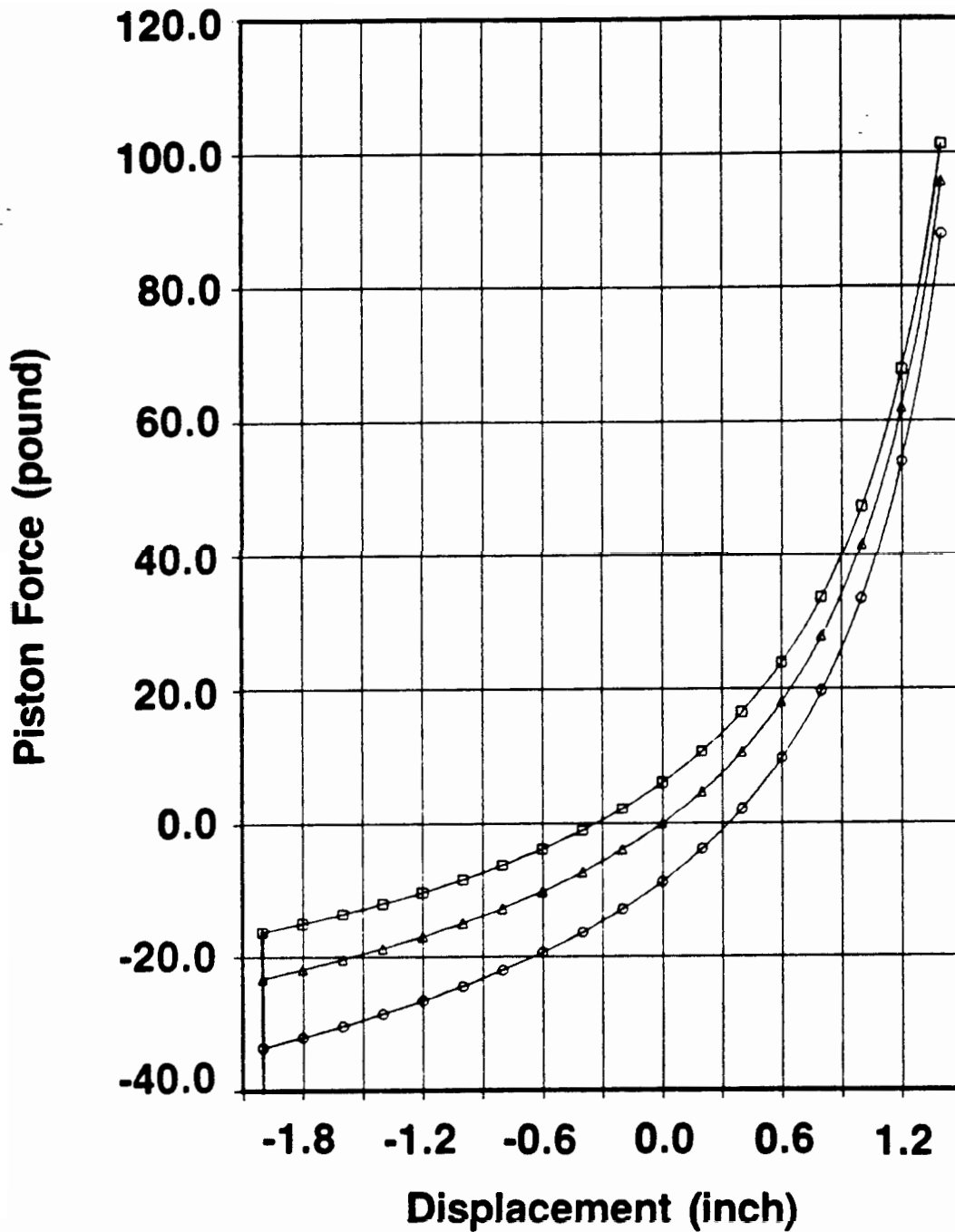


Figure 3. The Force-Displacement Curve of the Piston;

- \square -- $\Delta\delta = -1$ inch
- Δ -- $\Delta\delta = 0$ inch
- \circ -- $\Delta\delta = 1$ inch

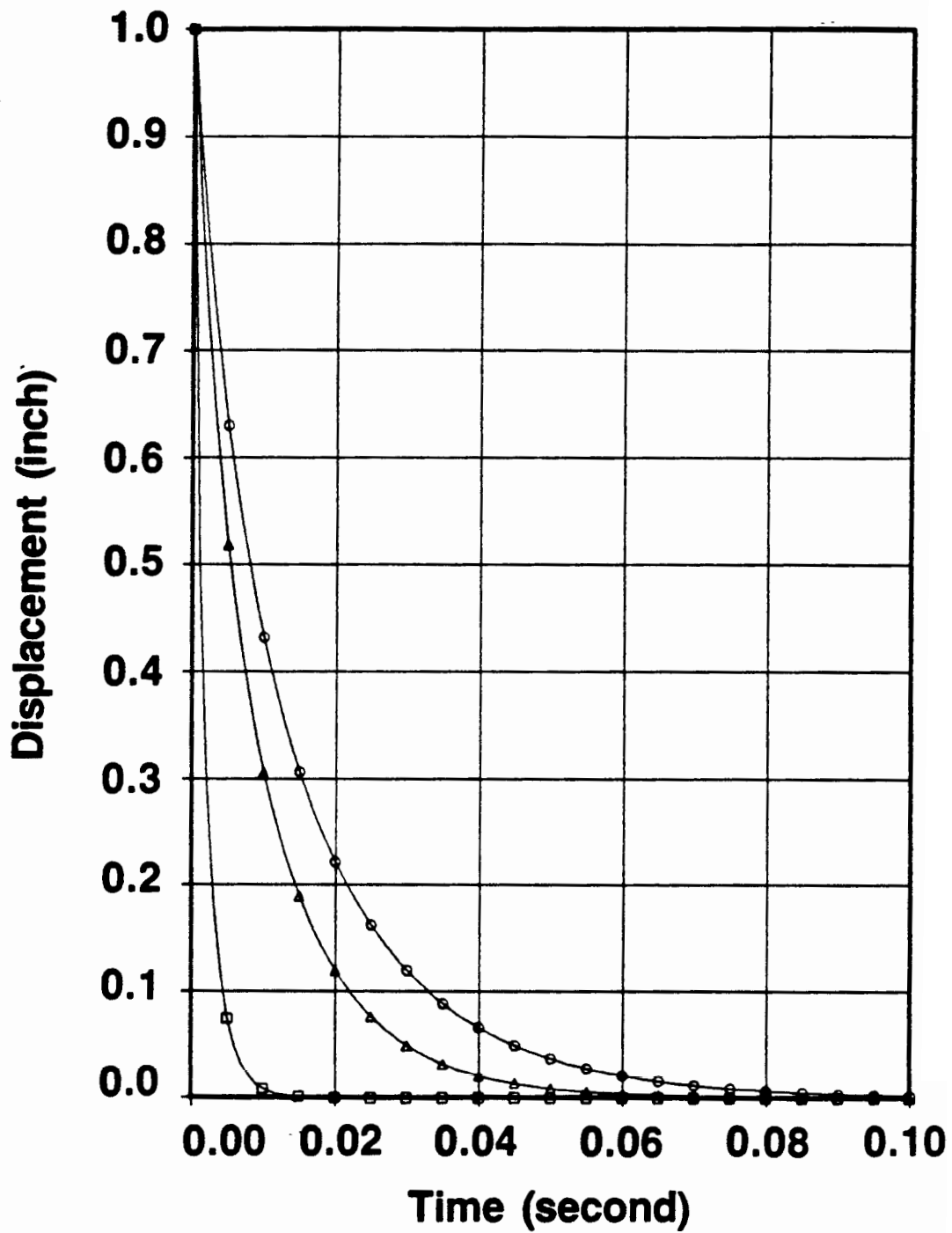


Figure 4. The Damping Effect of the Piston

□ $-\beta_2 = 0.2$, Δ $-\beta_2 = 1.0$, \circ $-\beta_2 = 1.5$

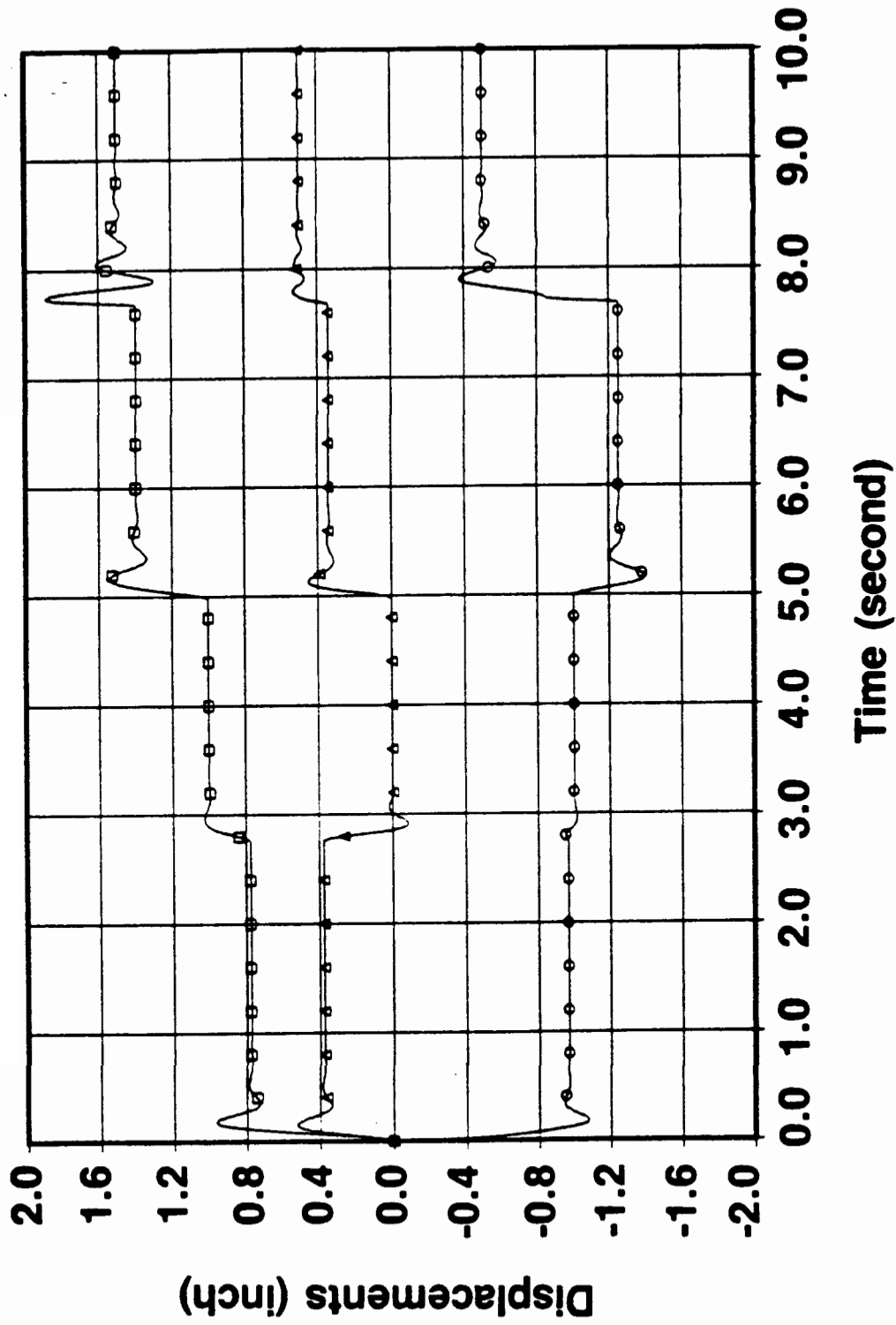


Figure 5. Position Control -- Displacements as Functions of Time,
 $\beta_2 = 1.5$ psi-sec/in. $\ast\ast 3$
 \square -- U_x , Δ -- U_y , \circ -- U_z

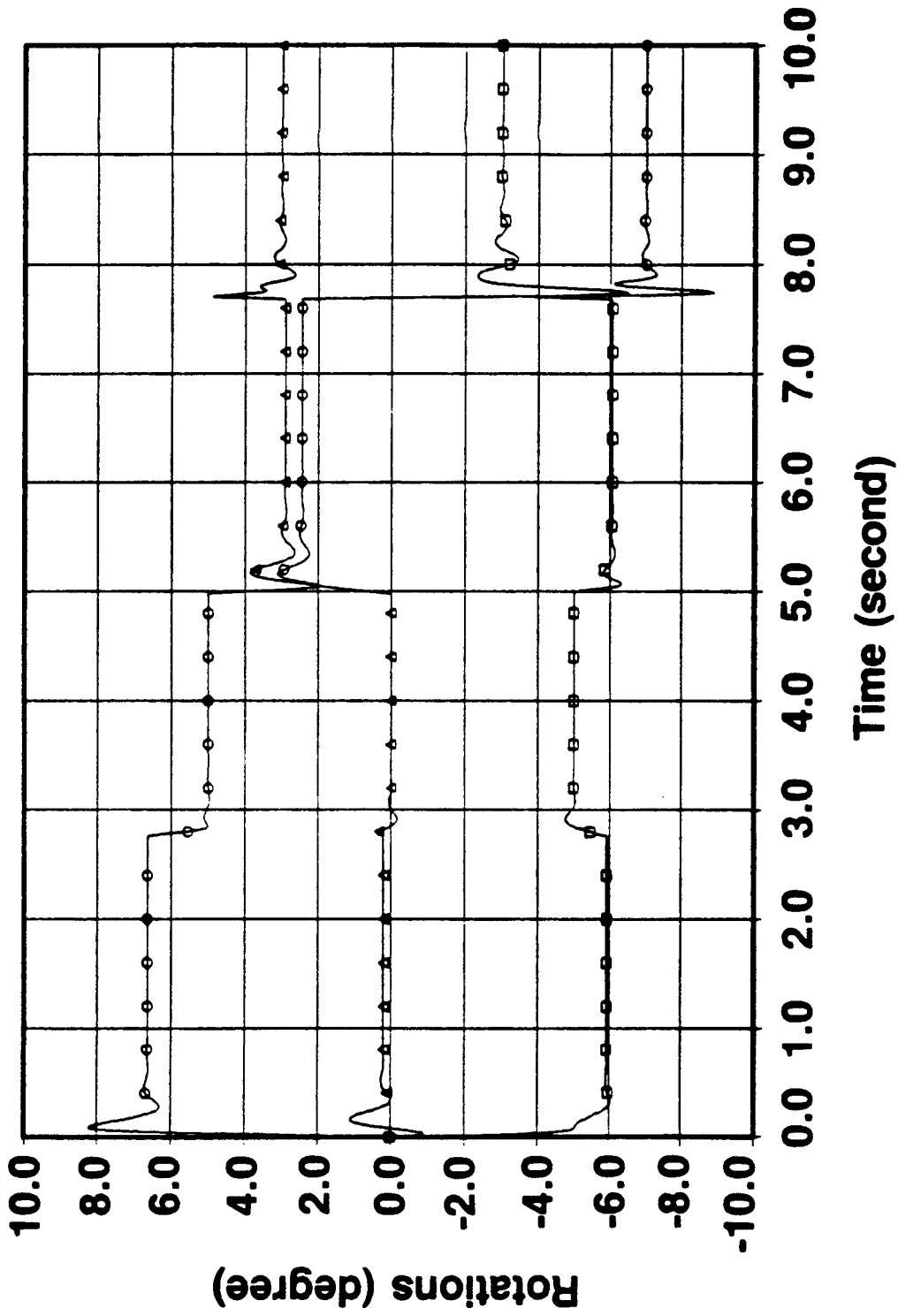


Figure 6. Position Control -- Rotations as Functions of Time,

$\beta_2 = 1.5 \text{ psi-sec/in.} \cdot \cdot 3$

□ --- θ_x , Δ --- θ_y , \circ --- θ_z

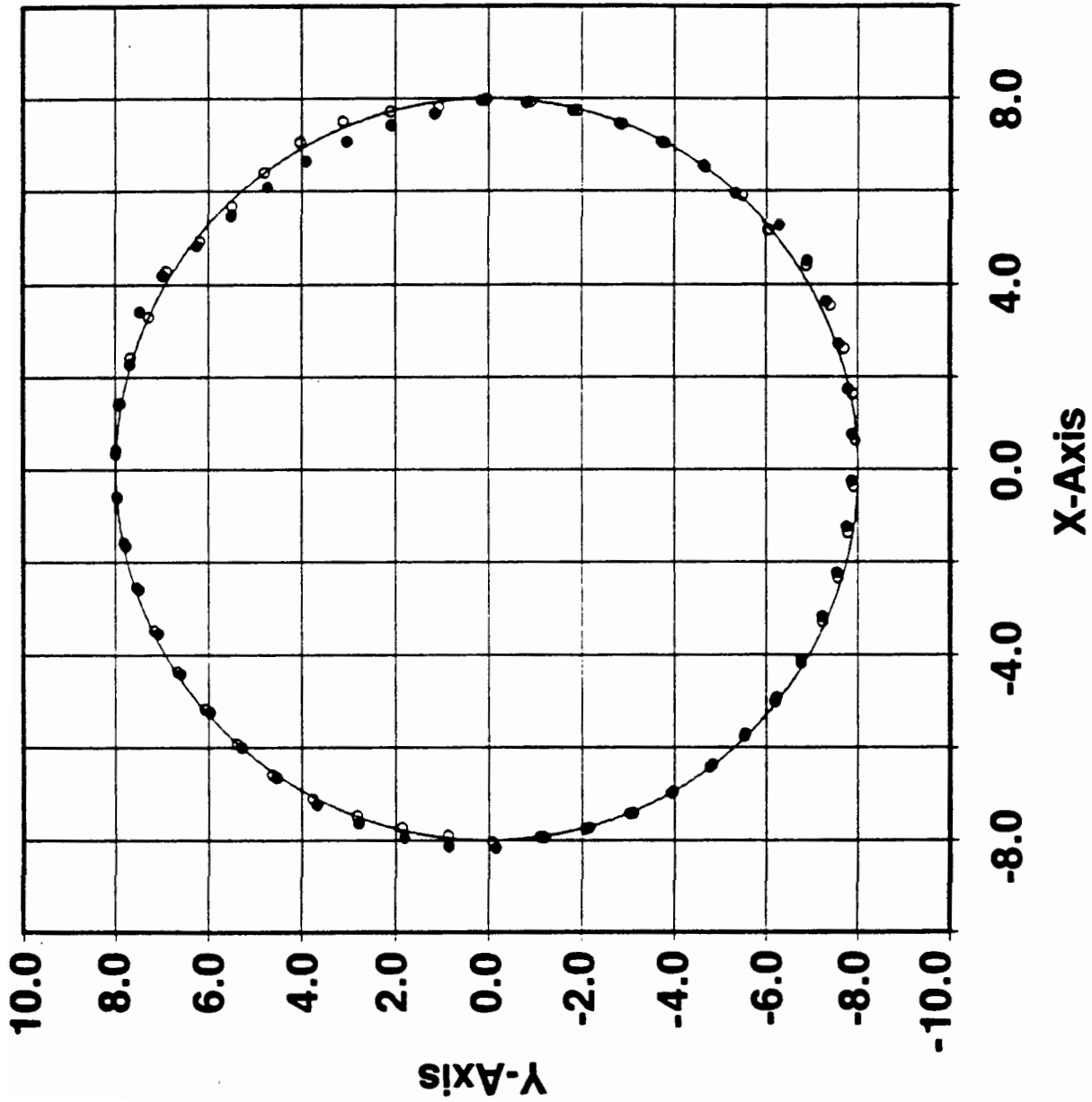


Figure 7. Path Tracing, Damping Coefficient $\beta_2 = 1.0$ psi-sec/in. $\ast\ast 3$

- --- T = 20 seconds
- --- T = 10 seconds

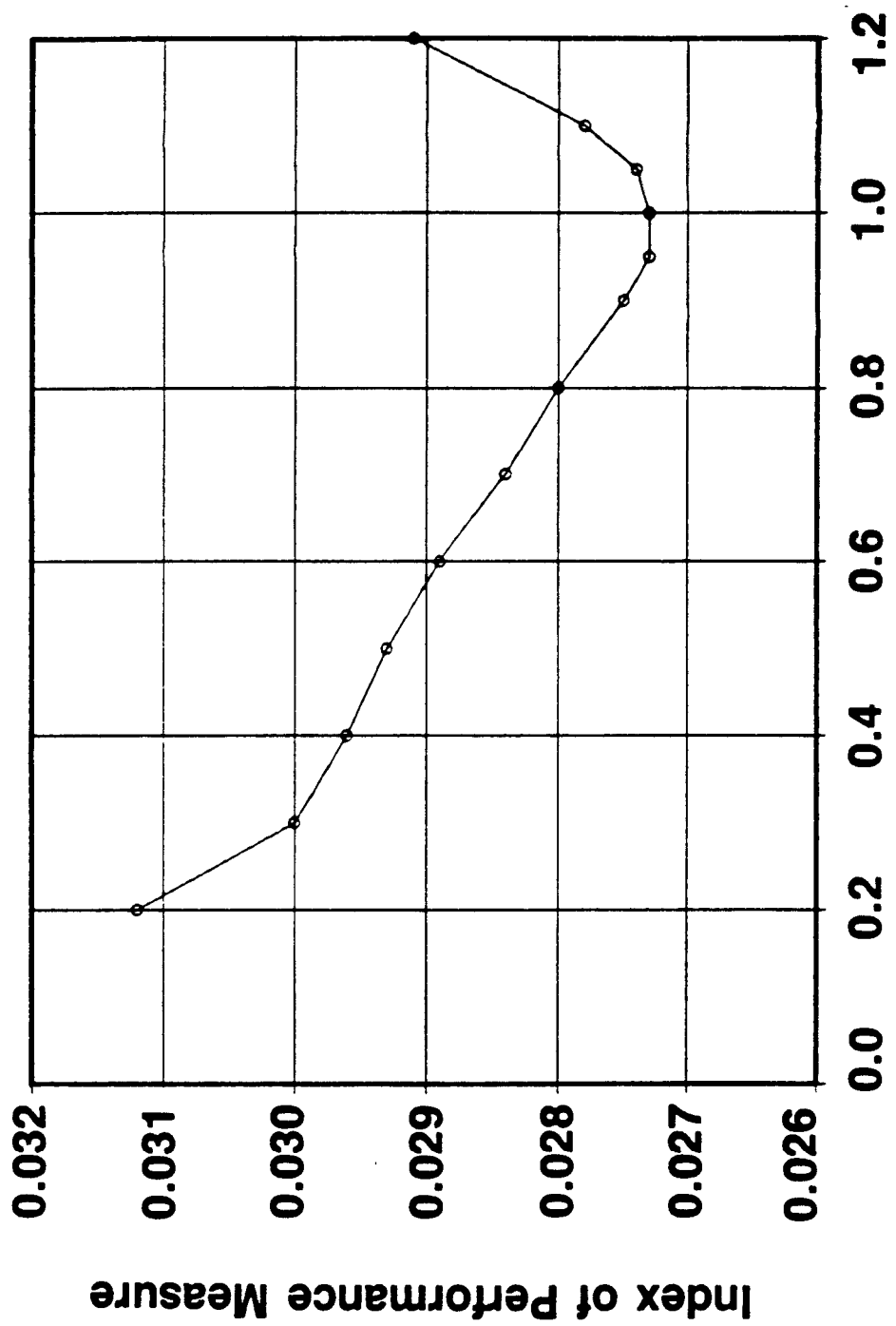


Figure 8. Index of Performance Measure as a Function of Damping Coefficient, T = 10 seconds

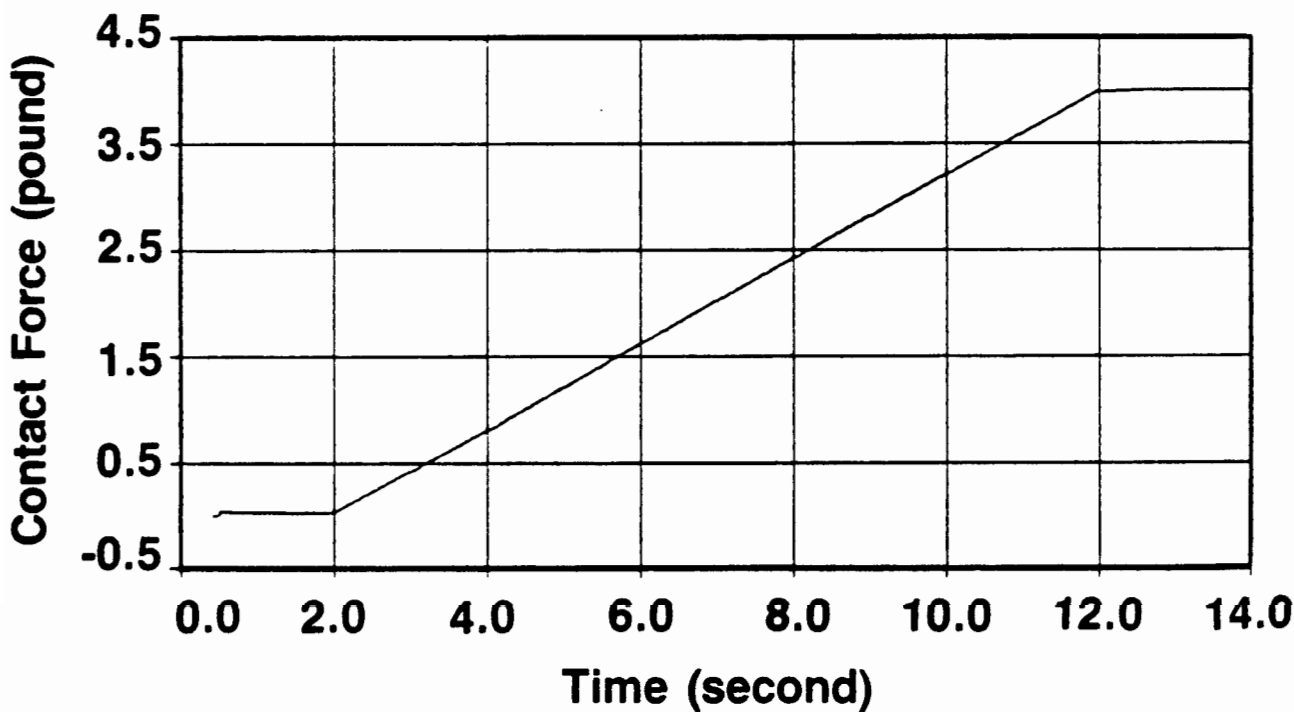
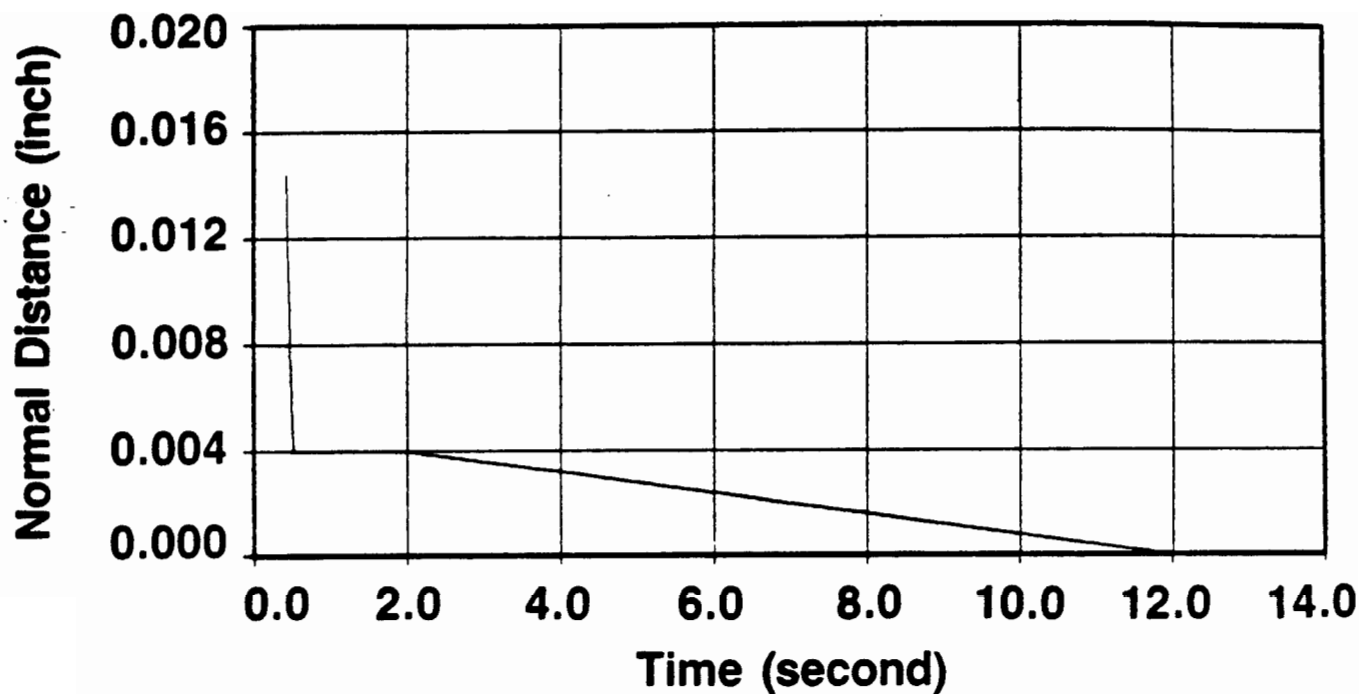


Figure 9. Force Control -- Normal Distance and Contact Force as Functions of Time, Damping Coefficient = 20 psi-sec/in.***3

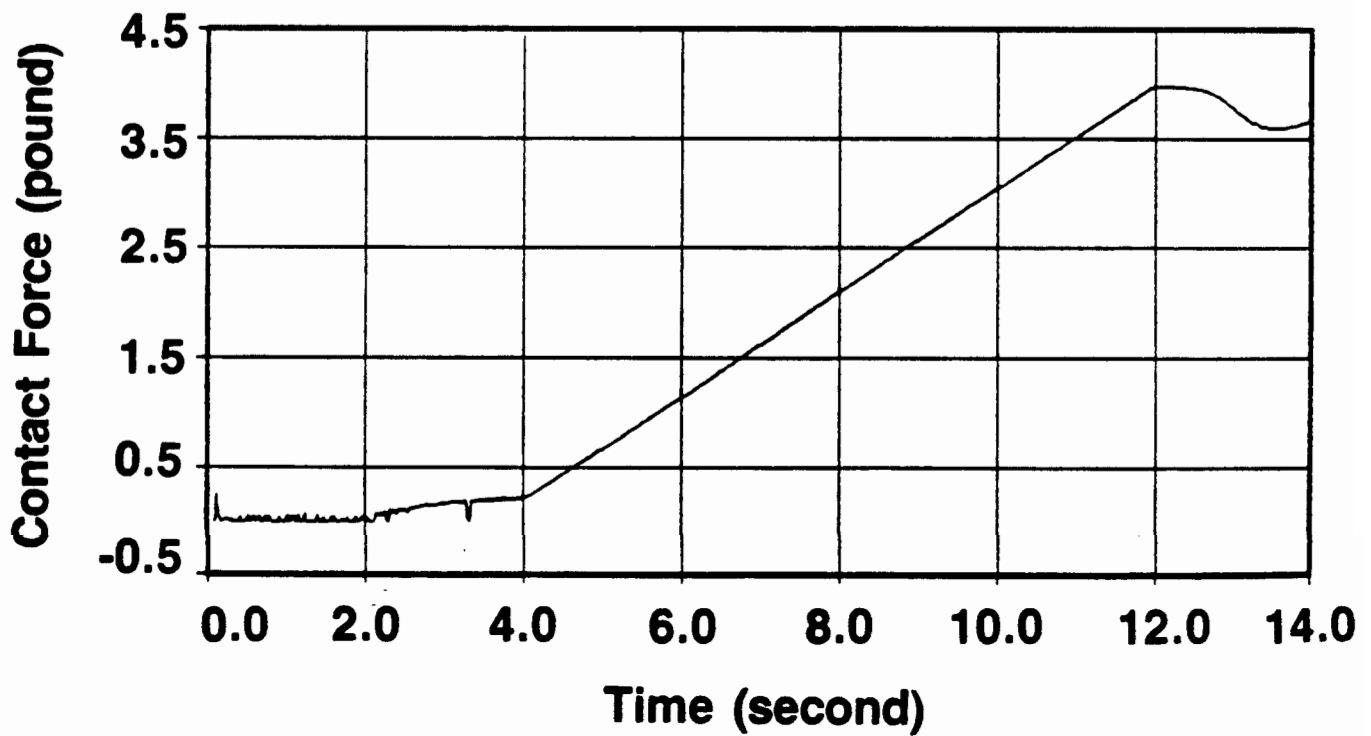
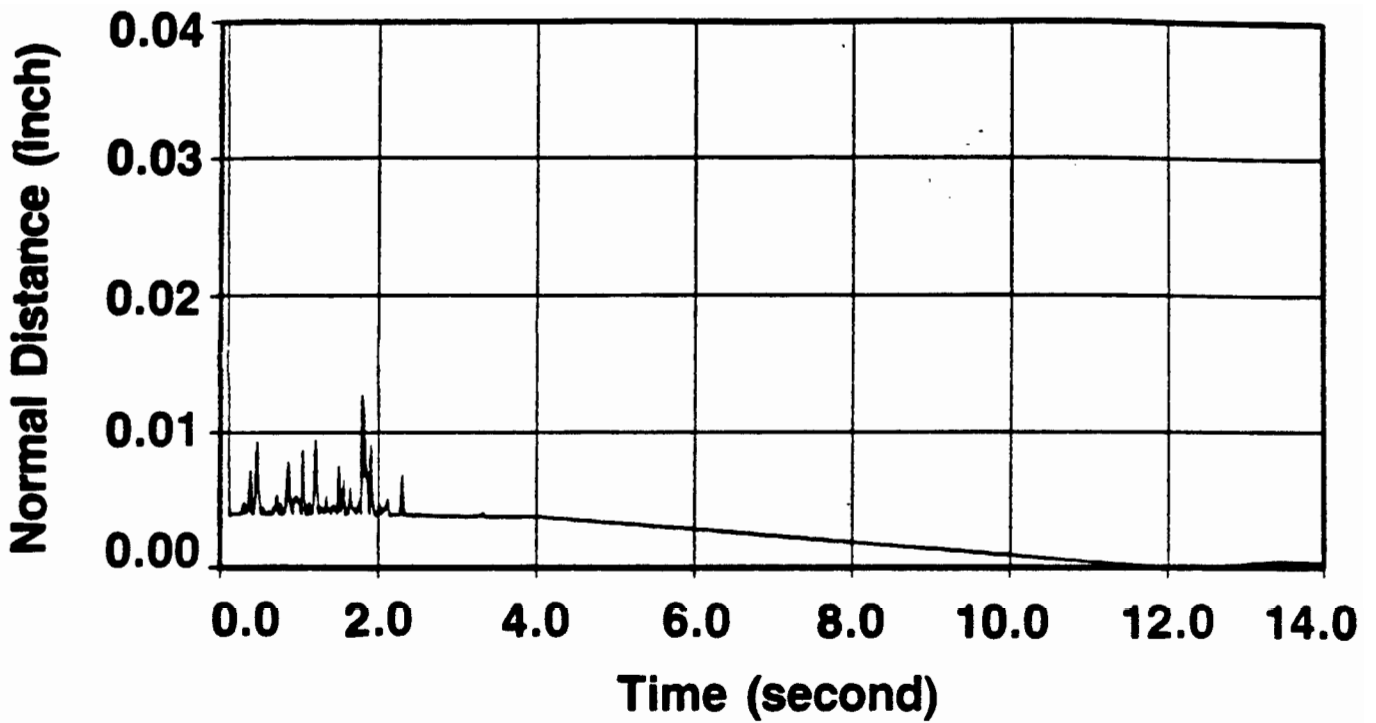


Figure 10. Force Control – Normal Distance and Contact Force as Functions of Time, Damping Coefficient = 5 psi-sec/in. **3